This is the accepted manuscript made available via CHORUS. The article has been published as:

Reporter-Spin-Assisted math xmlns="http://www.w3.org/1998/Math/MathML" display="inline" overflow="scroll">msub>mi>T/mi> mn>1/mn>/msub>/math> Relaxometry

Zhiran Zhang, Maxime Joos, Dolev Bluvstein, Yuanqi Lyu, and Ania C. Bleszynski Jayich

Phys. Rev. Applied **19**, L031004 — Published 16 March 2023

DOI: 10.1103/PhysRevApplied.19.L031004

Reporter-spin-assisted T_1 relaxometry

Zhiran Zhang,[1] Maxime Joos,[1] Dolev Bluvstein,[1,2] Yuanqi Lyu,[1,3] and Ania C. Bleszynski Jayich[1,*]

[1] *Department of Physics, University of California, Santa Barbara, California 93106, USA*
[2] *Department of Physics, Harvard University, Cambridge, Massachusetts 02138, USA*
[3] *Department of Physics, University of California, Berkeley, California 94720, USA*

A single spin quantum sensor can quantitatively detect and image fluctuating electromagnetic fields via their effect on the sensor spin's relaxation time, thus revealing important information about the target solid-state or molecular structures. However, the sensitivity and spatial resolution of spin relaxometry are often limited by the distance between the sensor and target. Here, we propose an alternative approach that leverages an auxiliary reporter spin in conjunction with a single spin sensor, a diamond nitrogen vacancy (NV) center. We show that this approach can realize a 100-fold measurement sensitivity improvement for realistic working conditions and we experimentally verify the proposed method using a single shallow NV center. Our work opens up a broad path of inquiry into a range of possible spin systems that can serve as relaxation sensors without the need for optical initialization and readout capabilities.

The detection of fluctuating electromagnetic fields lends important insight into the dynamics of solid-state systems, for example, the local current and spin fluctuations in magnetic and correlated electron systems [1–6], decoherence processes in quantum systems [7–11], and chemical and biological processes [12–14]. Single-spin quantum sensors constitute a powerful tool for detecting fluctuating fields; in a technique called relaxometry, fluctuating fields with a spectral component matched to the energy splitting of the sensor spin reduce the spin's relaxation time T_1 [15].

Nitrogen vacancy (NV) centers in diamond are a prominent example of a solid-state spin qubit sensor, exhibiting a wide temperature operating range, compatibility with biological and condensed matter systems, high sensitivity, and high spatial resolution. Relaxometry with NV centers has been used to probe magnetic fluctuations near the diamond surface to better understand surface-induced decoherence [8–11], detect spin waves in magnetic systems [16, 17], image local conductivity and current flow of condensed matter systems [18–21], perform spectroscopy of electronic spins [22], and detect magnetic nanoparticles [23] and magnetic ions [24–26]. The proximity of the sensor to its target is critical to achieving better spatial resolution and sensitivity, and becomes particularly important for relaxometry when targeting the detection of single spins (nuclear or electronic), as the dipolar magnetic fluctuation signal from a single spin die off as $1/r^6$, with r being the sensor-target separation [24, 27].

Bringing NV centers close to the diamond surface is one natural approach to reduce sensor-target separation for improved relaxometry. However, NV centers with high-grade spin and optical properties cannot be made arbitrarily shallow for many reasons: firstly, the yield rate of an implanted nitrogen atom forming an NV center declines dramatically near the surface [28], and secondly, near-surface NVs tend to exhibit increased charge instabilities [29–31] and shorter coherence times [10, 32]. Overcoming these challenges is an active area of study.

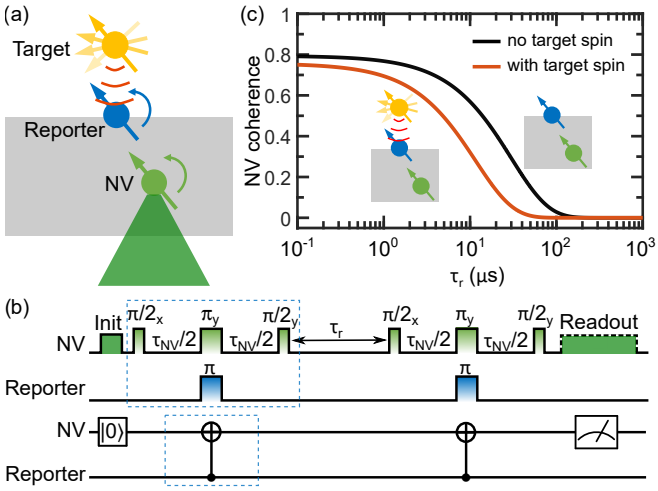

FIG. 1. (a) Schematic representation of the proposed experiment. The magnetic fluctuations (red contours) from a target spin (yellow) are detected by an optically addressable NV center (green) in diamond, through a change in the relaxation time $T_{1,R}$ of the reporter spin at the diamond surface. The close proximity of the reporter spin to the target spin amplifies the signal. (b) Pulse sequence and corresponding quantum circuit diagram (bottom) used for measuring $T_{1,R}$. After optical initialization of the NV center (dark green), microwave pulses control the spin states of NV center (light green) and reporter spin (blue), followed by optical readout of the NV (dark green).(c) Calculated NV coherence as a function of τ_r as measured by the pulse sequence shown in (b), for an NV 4.5 nm deep. In the absence of a target spin, the black curve shows the signal corresponding to the reporter spin's intrinsic T_1, 30 μs in this case. The red curve shows a faster decay when a nearby Gd^{3+} spin, 3 nm from the reporter spin in this case, reduces $T_{1,R}$ to 11.6 µs.

Here we propose an alternative approach that leverages an auxiliary spin that resides closer to, or even at, the diamond surface (Fig. 1(a)) to sense fluctuating fields.

* ania@physics.ucsb.edu

This reporter spin acts as the relaxation sensor, whereas a nearby NV center, comfortably deeper in the diamond, serves as a local optical readout of the reporter spin state [33, 34]. Compared to direct NV relaxometry, this method features improved sensitivity and spatial resolution while circumventing the reduced NV coherence and charge stability associated with the diamond surface. In essence, the main advantage of the reporter relaxometry method stems from the fact that the reporter translates an incoherent magnetic field signal, which decays as $1/r^6$, into a coherent magnetic signal emanating from the reporter spin with a $1/r^3$ dependence. Furthermore, the proposed approach offers access to an additional range of detection frequencies determined by the reporter spin's energy splitting. In this paper, we analytically examine the dependence of the relaxation signal on NV and reporter spin properties, finding a measurement sensitivity increase up to 100-fold compared to conventional NV relaxometry as relevant parameters are varied in real working conditions. For concreteness, we use a theoretical calculation and a simulation of scanning relaxometry to benchmark performance using a specific example of detecting and imaging a single Gadolinium (Gd^{3+}) ion, a commonly used spin label for bio-structural imaging, but we remark that the results are broadly applicable to other target systems. We then experimentally verify the proposed pulse sequence with a single NV center strongly coupled to a nearby reporter spin, whose relaxation time is tuned via a stochastic driving technique [35]. Finally, the challenges and future outlook of this proposed approach are discussed.

We consider a single reporter spin located at the diamond surface near a single NV center, as shown in Fig. 1(a). Although the reporter spin can come in any form, its primary requirement is a long intrinsic T_1. We note that single spins at the diamond surface have been detected with 100-μs-scale relaxation times at room temperature [36], which are sufficiently long for the protocols proposed here. For simplicity, we discuss the case of spin-1/2 reporter spins, but the analysis can be extended to systems with larger spins.

The proposed reporter-spin relaxometry protocol is shown in Fig. 1(b). This protocol probes the correlation time of the magnetic field signal produced by the reporter spin, which is equal to its relaxation time $T_{1,R}$, via its dipolar coupling to the NV using double electron electron resonance (DEER) techniques. The sequence constitutes a correlation measurement of the NV center's environment seen through the filter function set by the "xyy" Hahn echo NV pulse sequence in this case. Importantly, by matching τ_{NV} to the inverse of the NV-reporter dipolar spin coupling rate k_s, the sequence selectively probes the coupling between the reporter spin and NV. Therefore, the two separate "xyy" DEER sequences are equivalent to two CNOT gates in quantum circuit representation [37]. The correlation time of such coupling is then imprinted onto the NV coherence, which can be measured via differential photoluminescence readout of the NV center's spin state [11]. In effect, the NV center acts as a "flag" qubit whose state changes if the reporter spin flips during the correlation sequence [38, 39].

Figure 1(c) shows the expected signal for the example case of detecting a single Gd^{3+} spin, a spin label with a large electronic spin of $S = 7/2$ and fast GHz-scale dynamics [12, 40]. Ensembles of Gd^{3+} spins have been interfaced with and detected by NV centers [24, 26, 27, 41]. The Gd^{3+} produces a rapidly fluctuating magnetic field, which reduces the correlation time of the reporter spin and manifests as a faster NV population decay. The reduction in NV coherence is caused by the relaxation of reporter spin. The NV parameters used in the numerical calculations are experimentally measured on an implanted shallow NV (NV1) in a chemical vapor deposition-grown diamond sample. The parameters are $T_2 = 8.4\,\mu\mathrm{s}$, and $T_{1,\mathrm{NV}} = 3.5\,\mathrm{ms}$, and the NV depth is measured via proton NMR [43, 44] to be 4.5 nm. The reporter spin is assumed to be located on the diamond surface at a position where the dipolar coupling to the NV is maximized, $T_{1,R}$ is assumed to be $30\,\mu\mathrm{s}$, and τ_{NV} is set to 912 ns to match the inverse of the dipolar coupling strength k_s [34].

To quantitatively compare the performance of the proposed reporter-spin-assisted relaxometry protocol with direct NV relaxometry, we first define the sensitivity of a relaxometry measurement as the minimum number of spins detectable per $\sqrt{\mathrm{Hz}}$:

$$\eta = \frac{C_{\mathrm{SPN}}}{\sqrt{2}\Delta S}\sqrt{t_{\mathrm{seq}}}, \tag{1}$$

where ΔS is the change of the normalized signal due to the reduced $T_{1,R}$, C_{SPN} is the ratio between experimental measurement uncertainty and the spin projection noise limit, and t_{seq} is the total duration of the pulse sequence including the overhead time, such as the initialization and readout time. The sensitivity of NV relaxometry η_{NV} and sensitivity of reporter relaxometry η_{R} are computed separately using Eq. (1) with the corresponding ΔS and t_{seq} for each method respectively. In the supplementary material, we also discuss results when the sensitivity is defined as the minimum detectable magnetic noise $\delta\langle B_\perp^2\rangle$ [42].

We next outline the steps of the numerical calculation for reporter and NV relaxometry sensitivities. We first calculate how a target fluctuating magnetic field external to the diamond imprints itself on the relaxation time of a single spin, which can be either the NV center when using direct NV relaxometry or the reporter spin when using reporter-spin-assisted relaxometry [27, 45, 46]. For the expected change in T_1, $\Delta S(\tau_{\mathrm{r}})$ is calculated as shown in Fig. 1(c). Then using Eq. (1), the readout and measurement times are optimized to minimize η_{R} and η_{NV} for each case independently, and the sensitivity enhancement $\eta_{\mathrm{NV}}/\eta_{\mathrm{R}}$ is calculated. We assume the use of the spin-to-charge conversion (SCC) readout technique for all cases

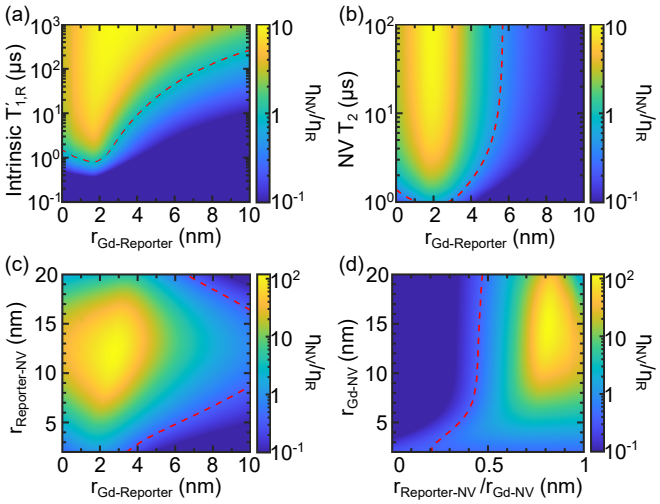

FIG. 2. Sensitivity improvement of reporter relaxometry over direct NV relaxometry for single Gd^{3+} spin detection. (a) Numerically calculated sensitivity enhancement ($\eta_{\mathrm{NV}}/\eta_{\mathrm{R}}$) as a function of the distance from the Gd^{3+} to reporter ($r_{\mathrm{Gd\text{-}Reporter}}$) and the intrinsic T_1 of the reporter. We assume NV $T_2 = 8.4\,\mu\mathrm{s}$, and NV depth is 4.5 nm. (b) $\eta_{\mathrm{NV}}/\eta_{\mathrm{R}}$ as a function of the distance from the single Gd^{3+} to the reporter, and the NV T_2. We assume reporter spin $T_{1,R} = 30\,\mu\mathrm{s}$, and NV depth is 4.5 nm. (c)(d) $\eta_{\mathrm{NV}}/\eta_{\mathrm{R}}$ as a function of the distances between NV, reporter, and the single Gd^{3+}. We assume NV $T_2 = 100\,\mu\mathrm{s}$ and reporter spin $T_{1,R} = 30\,\mu\mathrm{s}$. SCC readout technique is used here for both reporter relaxometry and NV relaxometry. The red dashed lines indicate $\eta_{\mathrm{NV}}/\eta_{\mathrm{R}} = 1$, where the sensitivities of two methods are equal.

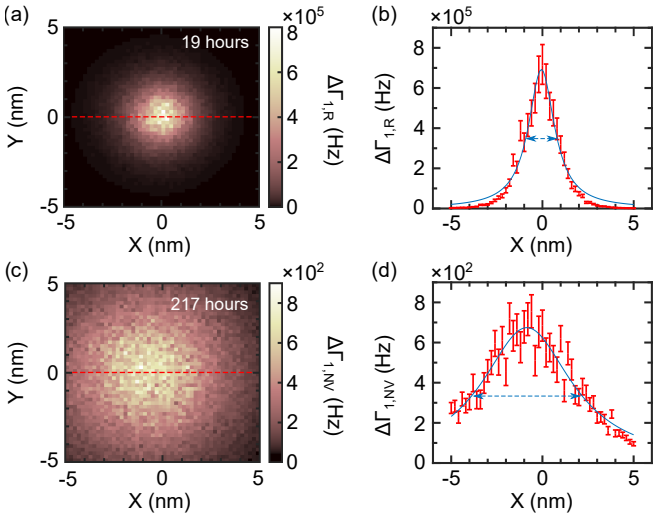

FIG. 3. A comparison of simulated scanning images of a single Gd^{3+} spin acquired by reporter relaxometry and direct NV relaxometry. (a) Reporter-spin assisted relaxometry image: plotted is the change of reporter relaxation rate, $\Delta\Gamma_{1,R}$, as the reporter spin is scanned in a plane 2 nm above a single Gd^{3+}. (b) A line-cut along the red dashed line in (a). (c) Direct NV relaxometry image plots the change of NV relaxation rate, $\Delta\Gamma_{1,\mathrm{NV}}$, as the NV center is scanned in a plane 6.5 nm above a single Gd^{3+}. (d) A line-cut of the red dashed line in (c). The reporter relaxometry image in (a) takes 19 hours compared to 217 hours for direct NV relaxometry imaging. These simulations target the same level of relative standard error for each pixel. The solid blue lines in (b) and (d) are Lorentzian fits, and the dashed lines with arrows indicate the FWHM. For both images, the NV $T_{1,\mathrm{NV}} = 3.5\,\mathrm{ms}$, $T_2 = 8.4\,\mu\mathrm{s}$, NV depth is 4.5 nm, and the reporter $T_{1,R} = 100\,\mu\mathrm{s}$.

here, where the readout noise level is experimentally verified on NV1 [47].

Figure 2 plots the sensitivity enhancement of the reporter spin relaxometry protocol over the direct NV relaxometry protocol, varying several parameters to highlight the situations in which reporter spins are an advantageous choice. The qualitative picture that emerges from the plots is that longer intrinsic reporter $T_{1,R}^{'}$, longer NV T_2, smaller reporter-Gd^{3+} separations, and deeper NV centers enhance the benefits of reporter relaxometry, culminating in a 100-fold sensitivity enhancement for a 10-15 nm deep NV with $T_2 = 100\,\mu\mathrm{s}$ and a Gd^{3+} spin located ∼3 nm above a reporter spin with $T_{1,R}^{'} = 30\,\mu\mathrm{s}$ (Fig. 2(c)(d)). We note that these are all experimentally confirmed values [11, 26, 30, 44]. A lower (higher) NV T_2 would shift the location of maximal sensitivity enhancement in Fig. 2(c) to smaller (larger) reporter-NV separations $r_{\mathrm{reporter\text{-}NV}}$, and reduce (enhance) the sensitivity enhancement value $\eta_{\mathrm{NV}}/\eta_{\mathrm{R}}$ (shown in our Supplementary Material Note 4 [42]). For each point calculated in Fig. 2, the readout and measurement times are optimized to minimize η_{R} and η_{NV} separately [42].

Reporter relaxometry can also be combined with scanning probe microscopy (SPM) [20, 23, 25, 48] to achieve better spatial resolution and provide faster imaging for a given sensitivity. In reporter-spin-assisted scanning relaxometry, a reporter spin is incorporated onto the apex of a diamond scanning probe tip with a nearby subsurface NV center and is scanned over an imaging target, spatially mapping the fluctuating fields emanating from the sample. In Fig. 3 we compare two simulated images of a single Gd^{3+} spin obtained using scanning reporter T_1 relaxometry (Fig. 3(a)) and direct scanning NV T_1 relaxometry (Fig. 3(c)). The change of the reporter's relaxation rate is plotted against its lateral position relative to the Gd^{3+} as it is scanned above the diamond surface. Noise at the level of $C_{\mathrm{SPN}} \approx 10$, as experimentally measured on NV1, is included. We utilize an adaptive measurement technique [20] that optimizes the parameters of the pulse sequence (τ_{r} and readout time) at each pixel. We also set the averaging time at each pixel to maintain a constant relative standard error of $\Delta\Gamma_1$, where $\Delta\Gamma_1 = 1/T_1 - 1/T_1^{'}$ is the change in relaxation induced by the Gd^{3+}. We find that reporter relaxometry shows a 11.4-fold overall measurement speed enhancement, and a 3.5-fold better spatial resolution (FWHM resolution) as seen by comparing the signals shown in Fig. 3. The FWHM of the signal peaks in Fig. 3(b)(d) are limited by the distance between the sensor and target spin.

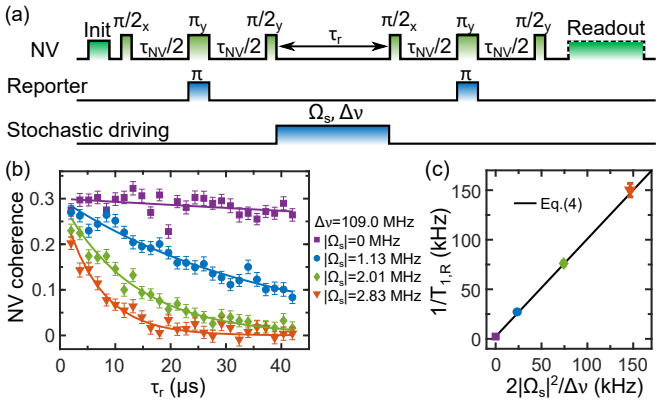

FIG. 4. Demonstration of reporter relaxometry with artificially reduced reporter spin correlation by stochastic driving. The measurement is performed with a single NV center that is strongly coupled to a nearby g=2 spin-1/2. (a) Pulse sequence of reporter relaxometry with additional stochastic driving of the reporter spin during τ_r. Incoherent spin dynamics caused by stochastic driving with Rabi frequency $|\Omega_s|$ and linewidth $\Delta\nu$ reduces $T_{1,R}$ of the reporter spin. (b) NV coherence for various stochastic driving powers, indicating reduced reporter spin auto-correlation with increased Ω_s. Solid lines are mono-exponential decay fits. (c) Extracted reporter spin relaxation rate as a function of $2|\Omega_s|^2/\Delta\nu$. Black solid line is the theoretical behavior expected from Eq. (2).

We now experimentally demonstrate the ability of the proposed sequence (Fig. 1(b)) to accurately detect the T_1 reduction of a reporter spin. In this experiment, we apply an external stochastic field [35] to a reporter spin located in close proximity to an NV center, thus emulating the effect of fluctuating fields produced by a sensing target. The polychromatic drive, spectrally centered on the reporter spin resonance, reduces the correlation time of the reporter spin by inducing incoherent spin dynamics; the induced relaxation rate is controlled by the amplitude and broadening of the engineered field:

$$\frac{1}{T_{1,R}} = \frac{1}{T'_{1,R}} + 2\frac{|\Omega_s|^2}{\Delta\nu}. \tag{2}$$

where $|\Omega_s|$ is the Rabi frequency of the stochastic drive, and $\Delta\nu$ is the full-width at half maximum linewidth of the Lorentzian spectrum of the drive. We implement the reporter-assisted relaxometry sequence (Fig. 4(a)) on a single shallow NV center (NV2) in diamond that is strongly coupled to a nearby g=2 reporter spin and we probe the correlation of the reporter spin while turning on stochastic driving centered at 888.0 MHz during τ_r [42]. Figure 4(b) shows the reduced correlation of the reporter spin mapped onto the NV coherence as the strength of the stochastic drive is increased. For negligible stochastic drive power ($|\Omega_s| = 0$ kHz), the observed correlation is governed by the intrinsic slow relaxation of the reporter spin, $T'_{1,R} \approx 1$ ms in this case. As the drive power is increased, the reporter spin's correlation time is reduced and dominated by its incoherently driven dynamics. Figure 4(c) shows the reporter spin decay rate extracted from a mono-exponential fit to the data in Fig. 4(b) as a function of $|\Omega_s|^2/\Delta\nu$. Experimental results agree quantitatively with the expected behavior of Eq. (2) demonstrating the suitability of the reporter spin-assisted relaxometry sequence.

Another benefit of reporter spin relaxometry is its ability to probe fluctuating fields in a different frequency range than direct NV relaxometry, in particular giving access to lower frequencies at moderate fields. Many noise baths (e.g. Lorentzian baths) produce stronger fluctuations at lower frequencies. Further, probing two distinct frequency ranges simultaneously gives more spectral information about the sensing target.

Our work opens up a broad path of inquiry into a range of possible reporter spin systems that can serve as relaxation sensors without the need for optical initialization and readout capabilities. While engineering single reporter spins at the diamond surface is challenging, there are several promising candidates. Naturally occurring surface spins located on the diamond surface have been detected and measured to have remarkably long $T_1 = 100\,\mu$s [32, 34, 36, 44, 49–51], though further work is necessary to confirm their microscopic origin and engineer their properties. Reporter spins can also be engineered via ion implantation or chemical synthesis and patterning of molecules [52, 53], ions encapsulated in fullerene [54], rare-earth ions, and radical spin labels [55, 56].

In conclusion, we propose a method that utilizes reporter spins in conjunction with optically addressable NV centers in diamond to improve the measurement sensitivity and spatial resolution of conventional NV T_1 relaxometry sensing and imaging. We quantitatively compare the sensitivity and spatial resolution of this method to conventional NV T_1 relaxometry, and find a wide range of parameter space in which reporter spin relaxometry provides substantial gains. Proof-of-principle experiments confirm the ability of the proposed sequence to quantitatively probe the relaxation of a single, dark reporter spin. This work motivates the development of engineered reporter spins and some candidates are proposed.

We thank Tian-Xing Zheng and Peter Maurer for helpful discussions. We gratefully acknowledge support from the US Department of Energy (BES grant No. DE-SC0019241) for surface spin studies, the DARPA DRINQS program (Agreement No. D18AC00014) for driving protocols, and the NSF Convergence Accelerator (Award No. 2040520) for relaxometry numerical calculations and simulations. We acknowledge the use of shared facilities of the National Science Foundation (NSF) Materials Research Science and Engineering Center (MRSEC) at UC Santa Barbara, DMR 1720256, and the NSF Quantum Foundry through Q-AMASE-i program award DMR-1906325. D.B. acknowledges support from the NSF Graduate Research Fellowship Program (grant DGE1745303) and The Fannie and John Hertz Foundation.

[1] R. S. Hayano, Y. J. Uemura, J. Imazato, N. Nishida, T. Yamazaki, and R. Kubo, Zero-and low-field spin relaxation studied by positive muons, Phys. Rev. B **20**, 850 (1979).

[2] K. Agarwal, R. Schmidt, B. Halperin, V. Oganesyan, G. Zaránd, M. D. Lukin, and E. Demler, Magnetic noise spectroscopy as a probe of local electronic correlations in two-dimensional systems, Phys. Rev. B **95**, 155107 (2017).

[3] B. Flebus and Y. Tserkovnyak, Quantum-Impurity Relaxometry of Magnetization Dynamics, Phys. Rev. Lett. **121**, 187204 (2018).

[4] J. Y. Khoo, F. Pientka, and I. Sodemann, The universal shear conductivity of Fermi liquids and spinon Fermi surface states and its detection via spin qubit noise magnetometry, New J. Phys. **23**, 113009 (2021).

[5] S. Chatterjee, P. E. Dolgirev, I. Esterlis, A. A. Zibrov, M. D. Lukin, N. Y. Yao, and E. Demler, Single-spin qubit magnetic spectroscopy of two-dimensional superconductivity, Phys. Rev. Res. **4**, L012001 (2022).

[6] P. E. Dolgirev, S. Chatterjee, I. Esterlis, A. A. Zibrov, M. D. Lukin, N. Y. Yao, and E. Demler, Characterizing two-dimensional superconductivity via nanoscale noise magnetometry with single-spin qubits, Phys. Rev. B **105**, 024507 (2022).

[7] R. J. Schoelkopf, A. A. Clerk, S. M. Girvin, K. W. Lehnert, and M. H. Devoret, Qubits as Spectrometers of Quantum Noise, in *Quantum Noise in Mesoscopic Physics* (Springer Netherlands, Dordrecht, 2003) pp. 175–203.

[8] T. Rosskopf, A. Dussaux, K. Ohashi, M. Loretz, R. Schirhagl, H. Watanabe, S. Shikata, K. M. Itoh, and C. L. Degen, Investigation of surface magnetic noise by shallow spins in diamond, Phys. Rev. Lett. **112**, 147602 (2014).

[9] Y. Romach, C. Müller, T. Unden, L. J. Rogers, T. Isoda, K. M. Itoh, M. Markham, A. Stacey, J. Meijer, S. Pezzagna, B. Naydenov, L. P. McGuinness, N. Bar-Gill, and F. Jelezko, Spectroscopy of surface-induced noise using shallow spins in diamond, Phys. Rev. Lett. **114**, 017601 (2015).

[10] B. A. Myers, A. Das, M. C. Dartiailh, K. Ohno, D. D. Awschalom, and A. C. Bleszynski Jayich, Probing surface noise with depth-calibrated spins in diamond, Phys. Rev. Lett. **113**, 027602 (2014).

[11] B. A. Myers, A. Ariyaratne, and A. C. Bleszynski Jayich, Double-Quantum Spin-Relaxation Limits to Coherence of Near-Surface Nitrogen-Vacancy Centers, Phys. Rev. Lett. **118**, 197201 (2017).

[12] P. Caravan, J. J. Ellison, T. J. McMurry, and R. B. Lauffer, Gadolinium(III) chelates as MRI contrast agents: Structure, dynamics, and applications, Chem. Rev. **99**, 2293 (1999).

[13] A. M. Raitsimring, C. Gunanathan, A. Potapov, I. Efremenko, J. M. L. Martin, D. Milstein, and D. Goldfarb, Gd 3 + Complexes as Potential Spin Labels for High Field Pulsed EPR Distance Measurements, J. Am. Chem. Soc. **129**, 14138 (2007).

[14] C. Li, R. Soleyman, M. Kohandel, and P. Cappellaro, SARS-CoV-2 Quantum Sensor Based on Nitrogen-Vacancy Centers in Diamond, Nano Lett. **22**, 43 (2022).

[15] C. L. Degen, F. Reinhard, and P. Cappellaro, Quantum sensing, Rev. Mod. Phys. **89**, 035002 (2017).

[16] T. Van Der Sar, F. Casola, R. Walsworth, and A. Yacoby, Nanometre-scale probing of spin waves using single-electron spins, Nat. Commun. **6**, 7886 (2015).

[17] C. Du, T. van der Sar, T. X. Zhou, P. Upadhyaya, F. Casola, H. Zhang, M. C. Onbasli, C. A. Ross, R. L. Walsworth, Y. Tserkovnyak, and A. Yacoby, Control and local measurement of the spin chemical potential in a magnetic insulator, Science **357**, 195 (2017).

[18] L. S. Langsjoen, A. Poudel, M. G. Vavilov, and R. Joynt, Electromagnetic fluctuations near thin metallic films, Phys. Rev. B **89**, 115401 (2014).

[19] S. Kolkowitz, A. Safira, A. A. High, R. C. Devlin, S. Choi, Q. P. Unterreithmeier, D. Patterson, A. S. Zibrov, V. E. Manucharyan, H. Park, and M. D. Lukin, Probing Johnson noise and ballistic transport in normal metals with a single-spin qubit, Science **347**, 1129 (2015).

[20] A. Ariyaratne, D. Bluvstein, B. A. Myers, and A. C. Bleszynski Jayich, Nanoscale electrical conductivity imaging using a nitrogen-vacancy center in diamond, Nat. Commun. **9**, 2406 (2018).

[21] T. I. Andersen, B. L. Dwyer, J. D. Sanchez-Yamagishi, J. F. Rodriguez-Nieva, K. Agarwal, K. Watanabe, T. Taniguchi, E. A. Demler, P. Kim, H. Park, and M. D. Lukin, Electron-phonon instability in graphene revealed by global and local noise probes, Science **364**, 154 (2019).

[22] L. T. Hall, P. Kehayias, D. A. Simpson, A. Jarmola, A. Stacey, D. Budker, and L. C. Hollenberg, Detection of nanoscale electron spin resonance spectra demonstrated using nitrogen-vacancy centre probes in diamond, Nat. Commun. **7**, 10211 (2016).

[23] D. Schmid-Lorch, T. Häberle, F. Reinhard, A. Zappe, M. Slota, L. Bogani, A. Finkler, and J. Wrachtrup, Relaxometry and Dephasing Imaging of Superparamagnetic Magnetite Nanoparticles Using a Single Qubit, Nano Lett. **15**, 4942 (2015).

[24] S. Steinert, F. Ziem, L. T. Hall, A. Zappe, M. Schweikert, N. Götz, A. Aird, G. Balasubramanian, L. Hollenberg, and J. Wrachtrup, Magnetic spin imaging under ambient conditions with sub-cellular resolution, Nat. Commun. **4**, 1607 (2013).

[25] M. Pelliccione, B. A. Myers, L. M. A. Pascal, A. Das, and A. C. Bleszynski Jayich, Two-dimensional nanoscale imaging of gadolinium spins via scanning probe relaxometry with a single spin in diamond, Phys. Rev. Appl. **2**, 054014 (2014).

[26] A. O. Sushkov, N. Chisholm, I. Lovchinsky, M. Kubo, P. K. Lo, S. D. Bennett, D. Hunger, A. Akimov, R. L. Walsworth, H. Park, and M. D. Lukin, All-optical sensing of a single-molecule electron spin, Nano Lett. **14**, 6443 (2014).

[27] J. P. Tetienne, T. Hingant, L. Rondin, A. Cavaillès, L. Mayer, G. Dantelle, T. Gacoin, J. Wrachtrup, J. F. Roch, and V. Jacques, Spin relaxometry of single nitrogen-vacancy defects in diamond nanocrystals for magnetic noise sensing, Phys. Rev. B **87**, 235436 (2013).

[28] S. Pezzagna, B. Naydenov, F. Jelezko, J. Wrachtrup, and J. Meijer, Creation efficiency of nitrogen-vacancy centres in diamond, New J. Phys. **12**, 065017 (2010).

[29] L. Rondin, G. Dantelle, A. Slablab, F. Grosshans, F. Treussart, P. Bergonzo, S. Perruchas, T. Gacoin, M. Chaigneau, H. C. Chang, V. Jacques, and J. F. Roch, Surface-induced charge state conversion of nitrogen-vacancy defects in nanodiamonds, Phys. Rev. B **82**, 115449 (2010).

[30] D. Bluvstein, Z. Zhang, and A. C. Bleszynski Jayich, Identifying and Mitigating Charge Instabilities in Shallow Diamond Nitrogen-Vacancy Centers, Phys. Rev. Lett. **122**, 076101 (2019).

[31] Z. Yuan, M. Fitzpatrick, L. V. H. Rodgers, S. Sangtawesin, S. Srinivasan, and N. P. de Leon, Charge state dynamics and optically detected electron spin resonance contrast of shallow nitrogen-vacancy centers in diamond, Phys. Rev. Res. **2**, 033263 (2020).

[32] S. Sangtawesin, B. L. Dwyer, S. Srinivasan, J. J. Allred, L. V. H. Rodgers, K. De Greve, A. Stacey, N. Dontschuk, K. M. O'Donnell, D. Hu, D. A. Evans, C. Jaye, D. A. Fischer, M. L. Markham, D. J. Twitchen, H. Park, M. D. Lukin, and N. P. de Leon, Origins of Diamond Surface Noise Probed by Correlating Single-Spin Measurements with Surface Spectroscopy, Phys. Rev. X **9**, 031052 (2019).

[33] M. Schaffry, E. M. Gauger, J. J. L. Morton, and S. C. Benjamin, Proposed spin amplification for magnetic sensors employing crystal defects, Phys. Rev. Lett. **107**, 207210 (2011).

[34] A. O. Sushkov, I. Lovchinsky, N. Chisholm, R. L. Walsworth, H. Park, and M. D. Lukin, Magnetic resonance detection of individual proton spins using quantum reporters, Phys. Rev. Lett. **113**, 197601 (2014).

[35] M. Joos, D. Bluvstein, Y. Lyu, D. M. Weld, and A. Bleszynski Jayich, Protecting qubit coherence by spectrally engineered driving of the spin environment, Npj Quantum Inf. **8**, 47 (2021).

[36] B. L. Dwyer, L. V. H. Rodgers, E. K. Urbach, D. Bluvstein, S. Sangtawesin, H. Zhou, Y. Nassab, M. Fitzpatrick, Z. Yuan, K. De Greve, E. L. Peterson, H. Knowles, T. Sumarac, J.-P. Chou, A. Gali, V. Dobrovitski, M. D. Lukin, and N. P. de Leon, Probing spin dynamics on diamond surfaces using a single quantum sensor, PRX Quantum **3**, 040328 (2022).

[37] K. Rezai, S. Choi, M. D. Lukin, and A. O. Sushkov, Probing dynamics of a two-dimensional dipolar spin ensemble using single qubit sensor, (2022), arXiv:2207.10688.

[38] R. Chao and B. W. Reichardt, Quantum Error Correction with Only Two Extra Qubits, Phys. Rev. Lett. **121**, 050502 (2018).

[39] A. Laraoui, F. Dolde, C. Burk, F. Reinhard, J. Wrachtrup, and C. A. Meriles, High-resolution correlation spectroscopy of 13C spins near a nitrogen-vacancy centre in diamond, Nat. Commun. **4**, 1651 (2013).

[40] D. Goldfarb, Gd3+ spin labeling for distance measurements by pulse EPR spectroscopy, Phys. Chem. Chem. Phys. **16**, 9685 (2014).

[41] M. Pelliccione, A. Jenkins, P. Ovartchaiyapong, C. Reetz, E. Emmanouilidou, N. Ni, and A. C. Bleszynski Jayich, Scanned probe imaging of nanoscale magnetism at cryogenic temperatures with a single-spin quantum sensor, Nat. Nanotechnol. **11**, 700 (2016).

[42] See Supplemental Material at [URL will be inserted by publisher] for details on sample information, model of reporter relaxometry, numerical calculation, additional data, and analysis.

[43] L. M. Pham, S. J. DeVience, F. Casola, I. Lovchinsky, A. O. Sushkov, E. Bersin, J. Lee, E. Urbach, P. Cappellaro, H. Park, A. Yacoby, M. Lukin, and R. L. Walsworth, NMR technique for determining the depth of shallow nitrogen-vacancy centers in diamond, Phys. Rev. B **93**, 045425 (2016).

[44] D. Bluvstein, Z. Zhang, C. A. McLellan, N. R. Williams, and A. C. Bleszynski Jayich, Extending the Quantum Coherence of a Near-Surface Qubit by Coherently Driving the Paramagnetic Surface Environment, Phys. Rev. Lett. **123**, 146804 (2019).

[45] C. P. Slichter, *Principles of magnetic resonance*, 3rd ed. (Springer Berlin, Heidelberg, 1990).

[46] H. K. Kim, G. H. Lee, T. J. Kim, and Y. Chang, Determination of correlation times of new paramagnetic gadolinium MR contrast agents by EPR and 17O NMR, Bull. Korean Chem. Soc. **30**, 849 (2009).

[47] B. J. Shields, Q. P. Unterreithmeier, N. P. de Leon, H. Park, and M. D. Lukin, Efficient Readout of a Single Spin State in Diamond via Spin-to-Charge Conversion, Phys. Rev. Lett. **114**, 136402 (2015).

[48] A. Finco, A. Haykal, R. Tanos, F. Fabre, S. Chouaieb, W. Akhtar, I. Robert-Philip, W. Legrand, F. Ajejas, K. Bouzehouane, N. Reyren, T. Devolder, J. P. Adam, J. V. Kim, V. Cros, and V. Jacques, Imaging non-collinear antiferromagnetic textures via single spin relaxometry, Nat. Commun. **12**, 767 (2021).

[49] B. Grotz, J. Beck, P. Neumann, B. Naydenov, R. Reuter, F. Reinhard, F. Jelezko, J. Wrachtrup, D. Schweinfurth, B. Sarkar, and P. Hemmer, Sensing external spins with nitrogen-vacancy diamond, New J. Phys. **13**, 055004 (2011).

[50] M. S. Grinolds, M. Warner, K. De Greve, Y. Dovzhenko, L. Thiel, R. L. Walsworth, S. Hong, P. Maletinsky, and A. Yacoby, Subnanometre resolution in three-dimensional magnetic resonance imaging of individual dark spins, Nat. Nanotechnol. **9**, 279 (2014).

[51] A. Stacey, N. Dontschuk, J. P. Chou, D. A. Broadway, A. K. Schenk, M. J. Sear, J. P. Tetienne, A. Hoffman, S. Prawer, C. I. Pakes, A. Tadich, N. P. de Leon, A. Gali, and L. C. Hollenberg, Evidence for Primal sp 2 Defects at the Diamond Surface: Candidates for Electron Trapping and Noise Sources, Adv. Mater. Interfaces **6**, 1801449 (2019).

[52] J. J. L. Morton, A. M. Tyryshkin, A. Ardavan, K. Porfyrakis, S. A. Lyon, and G. A. D. Briggs, Environmental effects on electron spin relaxation in N@ C60, Phys. Rev. B **76**, 085418 (2007).

[53] K. Bader, D. Dengler, S. Lenz, B. Endeward, S. D. Jiang, P. Neugebauer, and J. Van Slageren, Room temperature quantum coherence in a potential molecular qubit, Nat. Commun. **5**, 5304 (2014).

[54] D. Pinto, D. Paone, B. Kern, T. Dierker, R. Wieczorek, A. Singha, D. Dasari, A. Finkler, W. Harneit, J. Wrachtrup, and K. Kern, Readout and control of an endofullerene electronic spin, Nat. Commun. **11**, 6405 (2020).

[55] M. Kveder, D. Merunka, M. Jokić, and B. Rakvin, Low-temperature electron-spin relaxation in the crystalline and glassy states of solid ethanol, Phys. Rev. B **77**, 094202 (2008).

[56] F. Shi, F. Kong, P. Zhao, X. Zhang, M. Chen, S. Chen, Q. Zhang, M. Wang, X. Ye, Z. Wang, Z. Qin, X. Rong, J. Su, P. Wang, P. Z. Qin, and J. Du, Single-DNA electron spin resonance spectroscopy in aqueous solutions, Nat. Methods **15**, 697 (2018).